

University of Warwick institutional repository: <http://go.warwick.ac.uk/wrap>

This paper is made available online in accordance with publisher policies. Please scroll down to view the document itself. Please refer to the repository record for this item and our policy information available from the repository home page for further information.

To see the final version of this paper please visit the publisher's website. Access to the published version may require a subscription.

Author(s): Ngo Minh Toan, Davide Marenduzzo, and Cristian Micheletti

Article Title: Inferring the Diameter of a Biopolymer from Its Stretching Response

Year of publication: 2005

Link to published version: <http://dx.doi.org/10.1529/biophysj.104.058081>

Publisher statement: None

# Inferring the Diameter of a Biopolymer from Its Stretching Response

Ngo Minh Toan,<sup>\*†</sup> Davide Marenduzzo,<sup>‡§</sup> and Cristian Micheletti<sup>\*</sup>

<sup>\*</sup>International School for Advanced Studies (S.I.S.S.A.) and the Istituto Nazionale Fisica della Materia, 34014 Trieste, Italy;

<sup>†</sup>Institute of Physics, Hanoi, Vietnam; <sup>‡</sup>The Rudolf Peierls Centre for Theoretical Physics, Oxford University, Oxford OX1 3NP, United Kingdom; and <sup>§</sup>Mathematics Institute, University of Warwick, Coventry CV4 7AL, United Kingdom

**ABSTRACT** We investigate the stretching response of a thick polymer model by means of extensive stochastic simulations. The computational results are synthesized in an analytic expression that characterizes how the force versus elongation curve depends on the polymer structural parameters: its thickness and granularity (spacing of the monomers). The expression is used to analyze experimental data for the stretching of various different types of biopolymers: polypeptides, polysaccharides, and nucleic acids. Besides recovering elastic parameters (such as the persistence length) that are consistent with those obtained from standard entropic models, the approach allows us to extract viable estimates for the polymers diameter and granularity. This shows that the basic structural polymer features have such a profound impact on the elastic behavior that they can be recovered with the sole input of stretching measurements.

## INTRODUCTION

In the past decade, remarkable technological progress has allowed experiments where single polymers are manipulated by means of optical or magnetic tweezers, microneedles, or atomic force microscopes (1–4). These micromanipulation techniques were used to characterize with great accuracy how various biopolymers such as DNA, proteins, and polysaccharides elongate under the action of a stretching force (4–14). The wealth of collected experimental data has constituted and still represents an invaluable and challenging benchmark for theoretical approaches to the problem (15–21). The typical models introduced to account for the observed stretching measurements rely on a description of the polymer as a one-dimensional curve with a certain persistence length. Two celebrated examples are provided by the freely jointed and the wormlike chain (FJC and WLC, respectively). Their widespread use reflects both their success in fitting experimental measurements and their simplicity of formulation. In fact, within the FJC model the polymer is described as a succession of phantom independent segments (15,22), whereas the WLC model relies on a description of the chain as a continuous curve characterized by a local bending rigidity (17,23,24).

In this study, we introduce a mesoscopic approach whereby a polymer is specified by its basic three-dimensional structural properties which, in turn, dictate how the chain responds under mechanical tension. This provides a novel view on the problem where the persistence length of the polymer (and its entire stretching curve) is not determined phenomenologically but is specified by fundamental structural parameters. As we shall discuss, this perspective opens the possibility to extract the fundamental structural param-

eters of biopolymers given the measurements of their stretching response.

The feasibility of the scheme outlined above relies on the possibility to model in an effective way how the polymer structural features impact on the elastic response. As a prerequisite, any such model should go beyond the one-dimensional schematization of the chain and capture its three-dimensional steric hindrance and the granularity associated with the monomeric units. Arguably, the simplest theoretical framework that possesses these requirements is the thick-chain (TC) model that has been recently developed in geometrical contexts motivated by the knotting of circular DNA (25–30). In the TC framework, a polymer is modeled as a discretised tube with a given thickness. The steric effects associated with the finite thickness are fully taken into account and introduce some strict constraints for the viable configurations that the chain can attain in the three-dimensional space. The implications of the selection in structure space operated by this steric criterion have been investigated in a variety of biophysical problems. In particular it has allowed elucidating the ubiquitous emergence of secondary motifs in proteins and the characterization of DNA knotting probabilities and DNA packaging thermodynamics (30–32). The diversity of these biological problems suggests that the TC model may be a sufficiently general framework to capture the stretching response of biopolymers with very different thicknesses and persistence lengths such as DNA, proteins, and polysaccharides.

A detailed discussion of the model is provided in the next section where we also discuss how its stretching response was characterized by computational means leading to a parametrization of the stretching curve in terms of the chain contour length, its thickness, and the length of the modular units (monomers). The resulting parametric expression is finally used to fit the experimental data on three different instances of biopolymers: the PEVK domain of protein (7–9), cellulose

*Submitted December 16, 2004, and accepted for publication April 4, 2005.*

Address reprint requests to Davide Marenduzzo, Oxford University, 1 Keble Road, OX1 3NP Oxford, UK. Fax: 44-0-1865-273947; E-mail: [davide@thphys.ox.ac.uk](mailto:davide@thphys.ox.ac.uk), or [davide@maths.warwick.ac.uk](mailto:davide@maths.warwick.ac.uk).

© 2005 by the Biophysical Society

0006-3495/05/07/80/07 \$2.00

doi: 10.1529/biophysj.104.058081

(11,33,34), and double-stranded DNA (5). It is shown that this approach allows extracting meaningful quantitative estimates of the effective thickness and modular granularity of the polymers. The persistence length implied by the structural parameters is consistent with that obtainable from the WLC or, according to the contexts, the FJC. In addition the overall quality of the fit of experimental data (measured in terms of  $\chi^2$ ) improves that achievable with either of the two reference entropic models.

## THEORY AND METHODS

To characterize the impact of a polymer's finite thickness on the stretching response, we shall view the polymer as a tube with a uniform circular section. Consistent with other studies, we define the chain thickness,  $\Delta$ , as the radius of the circular section and, furthermore, we coarse-grain the polymeric chain into a succession of discrete units equispaced at distance  $a$ . From a schematic point of view, the discretised TC can be thought of as consisting of tethered discs or oblate ellipsoids of radius  $\Delta$  and spacing  $a$ , as in Fig. 1 *a*.

Within the framework of elasticity theory, the elastic properties of a homogeneous tube are well characterized in the case where the tube is bent with respect to the straight reference configuration. If the bending angle is small, then the leading term in the elastic energy penalty has a quadratic dependence on the bending curvature. Already at this perturbative stage the thickness of a polymer, viewed as a uniformly dense tube, controls the elastic response since it determines the bending rigidity coefficient,  $\kappa_b$ . In fact, throughout a vast class of biopolymers,  $\kappa_b$  shows an approximate quartic dependence on  $\Delta$ , which implies that thermal excitations will be unable to excite appreciable local bends in sufficiently thick polymers (as microtubules (15)). Conversely, for smaller thickness, thermal excitations may cause appreciable deviations from the straight configuration. In this case the quadratic expansion of the elastic energy may be questioned since it does not penalize enough highly bent conformations. In the case of peptides, for example, the persistence length at room temperature is comparable with the nominal thickness (10,30, 35). From the quadratic approximation of the elastic energy, one would conclude that thermal excitations should easily

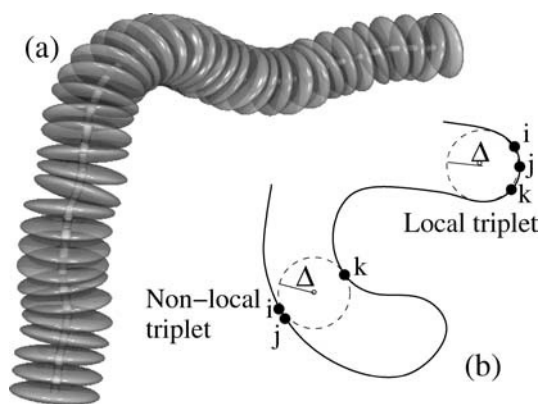


FIGURE 1 (a) Pictorial sketch of a discrete TC with thickness  $\Delta$  and granularity  $a$  (here,  $\Delta = 4a$ ). The finite thickness introduces steric constraints that forbid configurations where the chain self-intersects. (b) These constraints (which, e.g., for the chain of ellipsoids, may be implemented only with heavy computational expenditure) are more conveniently treated within the three-body prescription of the TC model. Within this approach, the centerline of a viable configuration is such that the radii,  $r_{ijk}$ , of the circles going through any triplet of points,  $i, j, k$ , on the curve are not smaller than  $\Delta$ .

introduce deformations corresponding to bending radii smaller than  $\Delta$ —a fact that should be strictly forbidden since it would lead to self-intersections. It therefore appears that a general mesoscopic model for the elasticity of biopolymers should take into account explicitly how the accessible conformational space is limited by the polymer finite thickness.

A theoretically appealing and computationally effective framework for treating the finite thickness in discrete polymer models was recently proposed in the context of ideal shapes of knots (25–29,36,37).

Physically, the finite thickness introduces restrictions on polymer chains that are both of local and nonlocal character. To avoid local self-intersection of the thick tube, the local radius of curvature must be no smaller than  $\Delta$ (25,27), as anticipated above. This introduces a limitation for the range of attainable values for the angle formed by two consecutive bonds of the discretised TC. Besides this local effect, there is also a nonlocal one: any two portions of the tube, at a finite arc-length separation, cannot interpenetrate (25,27). In traditional beads-and-strings models, it is only this second effect that is taken into account through a pairwise potential with a hard-core repulsion. Interestingly, one needs to go beyond pairwise interactions to account for the above mentioned effects in discretised polymer chains (38,39). In fact, the requirement on the local radius of curvature can be enforced by finding the radii of the circles going through any consecutive triplet of points and ensuring that each of them is greater than  $\Delta$ . The nonlocal effect can be addressed within the same framework by requiring that the minimum radius among circles going through any nonconsecutive triplet of points is also greater than  $\Delta$ . Indeed, the finite thickness,  $\Delta$ , of the discretised tube constrains the radii of the circles going through any triplet of distinct points to be greater than  $\Delta$  (see Fig. 1 *b* (27)).

The treatment followed here therefore focuses on thickness-induced effects that are complementary to those captured by the WLC. In fact, in the latter approach all three-dimensional arrangements of a chain are permitted but each structure carries a statistical weight that reflects its degree of local bending. In the TC model, the chain configurations that are incompatible with the finite polymer thickness are excluded but allowed configurations have the same statistical weight. The parameters that characterize a thick discrete chain within this model are three: the chain contour length,  $L_c$ , its thickness,  $\Delta$ , and the spacing,  $a$ , of the monomers which control the chain discretisation (granularity). It may be envisaged that a more powerful scheme would be to combine the WLC and TC by introducing a bending rigidity penalty among the physically allowed structures. This approach is certainly feasible though it requires the introduction of an additional parameter,  $\kappa_b$ , in the model. With the purpose of keeping the model as transparent as possible, we have restricted the analysis to the simplest formulation of the TC. This allows ascertaining how the reduction of configurational entropy operated by the thickness constraint affects a chain elastic response. Indeed, the restriction on the allowed conformational space is so severe that it is able to induce a finite persistence length,  $\xi_p$ , in the modeled chains.

At present, no exact expression for the dependence of  $\xi_p$  on  $\Delta$  and  $a$  is available. However, a useful approximate expression can be obtained by retaining only the local thickness constraints and neglecting the nonlocal ones. In this case, the only configurations available to the TC are those where the cosine of the angle formed by the tangent vectors of two consecutive chain bonds,  $\vec{t}_0$  and  $\vec{t}_1$ , is  $> 1 - a^2/2\Delta^2$ . The average value of their scalar product is, therefore,  $\langle \vec{t}_0 \cdot \vec{t}_1 \rangle = 1 - a^2/4\Delta^2$ . Subsequent bond tangent vectors,  $\vec{t}_n$ , will accumulate increasing deviations from the first tangent vector,  $\langle \vec{t}_0 \cdot \vec{t}_n \rangle = (1 - a^2/4\Delta^2)^n$ (31). One thus obtains that the persistence length induced by the local thickness constraint is

$$\xi_p = \frac{a}{\log\left(1 - \frac{a^2}{4\Delta^2}\right)}. \quad (1)$$

The previous analysis has strong analogies with the approach of Premilat and Hermans and of Flory and Conrad (40,41), which showed the profound influence of dihedral angle restrictions on the persistence length of poly-Gly and poly-Ala chains. The relevance of the thickness constraint for the modeling of biopolymer elasticity can be illustrated by applying Eq. 1 to the case of polypeptides and DNA. In the first case, the chain modularity is

intuitively suggested by the separation of consecutive  $C_\alpha$  atoms,  $a = 3.8 \text{ \AA}$ , whereas the typical polypeptide thickness obtained from previous studies is  $\Delta = 2.5 \text{ \AA}$ . This yields for  $\xi_p$  the value of  $0.55 \text{ nm}$ , which is in good agreement with the experimental value of  $0.4 \text{ nm}$  (10,35). For single- and double-stranded DNA,  $a$  is naturally taken as the nucleotide separation ( $a_{ss} = 0.55 \text{ nm}$ ) or the basepair spacing ( $a_{ds} = 0.34 \text{ nm}$ ), respectively, whereas the associated nominal values for  $\Delta$  based on structural determinations are  $\Delta_{ss} = 0.4 \text{ nm}$  and  $\Delta_{ds} = 1.25 \text{ nm}$ . For single-stranded DNA, this yields  $\xi_p^{ss} \approx 1.0 \text{ nm}$ , which is consistent with experimental determinations in solutions rich with monovalent counterions which screen the phosphate charges (23). For double-stranded DNA, one obtains  $\xi_p^{ds} \approx 19 \text{ nm}$ , which captures the correct order of magnitude of the experimentally determined one,  $\xi_p = 50 \text{ nm}$ . These examples, though based on the simplified local approximation for the persistence length, illustrate well how the basic elastic properties of various biopolymers can be influenced by their finite thickness.

In this study the complete characterization of the stretching response of a TC was obtained through extensive Monte Carlo simulations. The discretisation length,  $a$ , was taken as the unit length in the problem, and several values of  $\Delta/a$  were considered, ranging from the minimum allowed value of  $0.5$  (corresponding to the limit case where the oblate ellipsoids of Fig. 1 are spheres) to the value of  $4.0$ . This upper limit appears adequate in the present context since the largest nominal ratio for  $\Delta/a$  among the biopolymers considered here is achieved for dsDNA for which one has  $\Delta/a \approx 3.7$ . For each value of  $\Delta/a$  considered, the simulations were carried out on chains whose length was at least 10 times bigger than the persistence length estimated from Eq. 1. The relative elongation of the chain was calculated for increasing values of the applied stretching force (typically  $\sim 100$  distinct force values were considered). Starting from an arbitrary initial chain configuration, the exploration of the available structure space in the fixed-force ensemble was done by distorting conformations by means of pivot and crankshaft moves. The standard Metropolis algorithm was used to accept/reject the newly generated conformations. For each run, after equilibration, we measured the autocorrelation time and sampled a sufficient number of independent conformations to achieve a relative error of, at most,  $10^{-3}$  on the average chain elongation. For moderate or high forces, this typically entailed the collection of  $10^4$  independent structures, whereas a 10-fold increase of sampling was required at small forces due to the broad distribution of the end-to-end separation along the force direction.

From the simulations, several different stretching regimes could be identified in the elastic response of a TC. These are best discussed in connection with analogous regimes found in the FJC and WLC. For the former model, the functional dependence of the relative elongation,  $x$ , on the applied force,  $f$ , is given by

$$x = \coth\left(\frac{fb}{k_B T}\right) - \frac{k_B T}{fb}, \quad (2)$$

where  $b$  is the Kuhn length and  $k_B T$  is the thermal energy. The analogous characteristic relationship for the WLC is, instead, traditionally approximated as

$$f(x) = \frac{k_B T}{\xi_p} \left[ \frac{1}{4(1-x)^2} - \frac{1}{4} + x \right], \quad (3)$$

where  $\xi_p$  is the persistence length. It is apparent from both expressions that, at low force, the relative elongation,  $x$ , depends linearly on the applied force,  $f$ . This result holds also for the TC model. However, due to the self-avoidance of the TC, the Hookean relationship between  $f$  and  $x$  disappears in the limit of long polymer chains in favor of the Pincus regime,  $f \sim x^{1/(1-\nu)}$ ,  $\nu \sim 3/5$  being the critical exponent for self-avoiding polymers in three dimensions (16,22,42). For intermediate forces, the Pincus behavior is found to be followed by a second regime characterized by the same scaling relation found in the WLC at high forces,  $f \sim (1-x)^{-2}$ . As shown in Fig. 2, at still higher forces the same scaling relation found in the FJC is observed,  $f \sim (1-x)^{-1}$ . Physically, the first two regimes are determined by self-avoidance and chain stiffness or persistence length, whereas the last regime, present in the Kratky-Porod model, has recently been ascribed to the discrete nature of the chain (43–46).

Since the purpose of this study is to apply the TC model to contexts where experimental data are available, we have analyzed the numerical data with the purpose of extracting a single analytical expression which captures the observed functional dependence of  $f$  on  $\Delta$  and  $a$ . For any value of  $a$  and  $\Delta$ , the sought expression should reproduce the succession of the three regimes discussed above. Among several trial formulae we found, a posteriori, that the best interpolation was provided by the following expression,

$$f(x) = \frac{k_B T}{a(1-x)} \tanh\left(\frac{k_1 x^{3/2} + k_2 x^2 + k_3 x^3}{1-x}\right), \quad (4)$$

where the parametric dependence on  $\Delta$  and  $a$  is carried by the following expressions for the  $k_s$ ,

$$k_1^{-1} = -0.28394 + 0.76441\Delta/a + 0.31858\Delta^2/a^2, \quad (5)$$

$$k_2^{-1} = +0.15989 - 0.50503\Delta/a - 0.20636\Delta^2/a^2, \quad (6)$$

$$k_3^{-1} = -0.34984 + 1.23330\Delta/a + 0.58697\Delta^2/a^2. \quad (7)$$

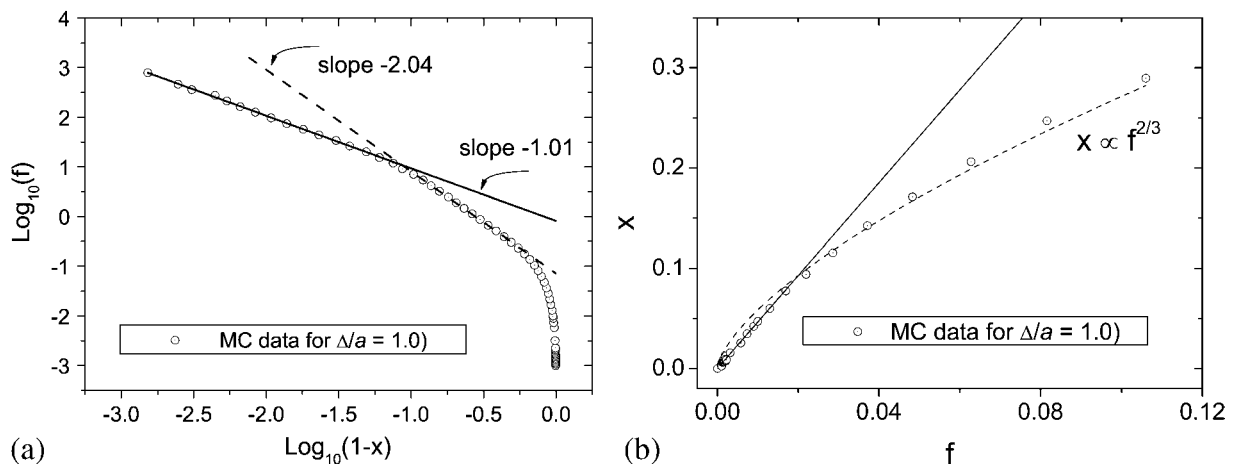


FIGURE 2 (a) Elongation versus force (expressed in units of  $k_B T/a$ ) for a chain of thickness  $\Delta/a = 1$ . Data points are presented in the  $(\log(1-x), \log(f))$  plane to highlight the WLC- and FJC-like regimes found at moderate and high forces. (b) Illustration of the low-force crossover from the Hookean regime,  $x \propto f$ , to the Pincus one,  $x \propto f^{2/3}$  for a chain of thickness  $\Delta/a = 1$  and  $N = 1200$  beads.

Within the explored ranges of  $\Delta$  and  $a$ , the relative extension obtained from Eq. 4 differs on average by 1% (and at most by 5%) from the true values at any value of the applied force. Through the analysis of the decay of tangent-tangent correlations in the configurations sampled in the absence of a stretching force, we also obtained the persistence length as a function of  $\Delta$  and  $a$ . For this quantity we found that expression of Eq. 1 already provides a very good approximation for the observed persistence length and found no need to correct it with other interpolation formulae.

In the discrete chain model considered here, the spacing of consecutive beads is constant along the chain. The application of arbitrarily large forces cannot, therefore, stretch a TC beyond its nominal contour length. This is true also for the FJC and WLC models described by Eqs. 2 and 3, since  $x$  cannot exceed 1 for any value of  $f$ . The property of inextensibility, though very natural and appealing, can make the models inadequate to capture the phenomenology of stretching at forces high enough to cause isomerization or structural transitions. Experiments on dsDNA, for example, have shown that forces  $>10$  pN can induce significant overstretching in the molecule (5). For polysaccharides such as dextran, a chair-to-boat transition occurs at forces around 700 pN, leaving a distinctive “bump” in the force versus elongation curves. The detailed description of how each type of biomolecule distorts at high stretching forces requires the use of ad hoc models and atomistic simulations thus going beyond the reach of simple phenomenological models (47). However, the simple inextensible models mentioned above can be generalized to describe, in a very satisfactory way, also the overstretching regime. This is accomplished by introducing an effective stretching modulus,  $K$ , controlling the elongation of the chain beyond its natural contour length (48). From a practical point of view, the relative extension,  $x$ , of Eqs. 2 and 3 is replaced by  $x(1 - f/K)$ . The same scheme could be adopted with the TC model too. In the interest of limiting the number of parameters in the theory, the focus of this work is limited to the inextensible model, which has, so far, been the reference case for TC models.

## RESULTS AND DISCUSSION

We have applied the TC results of Eq. 4 to interpret the experimental stretching curves of three types of biomolecules: the PEVK domain of titin, cellulose, and double-stranded DNA. Due to the inextensible nature of the TC model, it will be applied to fit data collected at forces below the known overstretching thresholds mentioned below. Our goal is twofold: on one hand we wish to verify the viability of the TC model in contexts where other entropic models are routinely used; on the other hand, we aim at extracting the relevant structural information (effective thickness and granularity) of the polymer from the experimental stretching curves.

For both purposes, a first useful benchmark is constituted by the PEVK domain of titin. The experimental data which we shall consider pertain to the atomic force measurements of Linke et al. (7) that were performed on heteropolymers comprising cardiac PEVK segments (each  $\sim 190$  residues long) in tandem with I27 domains. Some evidence has been previously presented in favor of the lack of structural organization in the PEVK domain. It therefore appears appropriate to model the PEVK elastic response as arising from entropic effects, as in a random coil (to which the PEVK domain has indeed been assimilated). The use of the WLC to fit the low-force data on the hetero-polyprotein returned a persistence length spanning the range 0.5–2.5 nm, the average being 0.9 nm (7).

Fig. 3 reproduces the stretching measurements on the polyprotein fitted by the TC model (assuming a constant error on the experimental force). To avoid the introduction of the spurious effects arising from the I27 mechanical unfolding (at 200 pN), in the fit of Fig. 3 and in all other sets of measurements made available to us we considered forces only up to 100 pN. For the specific example portrayed in Fig. 3, the contour length associated with the low-force part of the first peak resulted equal to  $147.6 \pm 0.3$  nm, fully consistent with the one determined from the WLC,  $148.1 \pm 0.1$  nm. The inferred structural parameters were, instead,  $a = 0.45 \pm 0.02$  nm,  $\Delta = 0.34 \pm 0.01$  nm, which from Eq. 1 yield a persistence length of  $0.77 \pm 0.03$  nm. Again, this value is consistent with the one obtained from the WLC on this particular sample,  $\xi_p^{\text{WLC}} = 0.76 \pm 0.02$  nm. The advantage of this approach is, however, that some insight is provided about the main structural parameters of the polymer. The average values of  $\Delta$  and  $a$  obtained from the fits of several experimental instances of (I27-PEVK) repeats gave  $\Delta = 2.63 \pm 0.36$  Å and  $a = 3.58 \pm 0.35$  Å. Both these parameters appear to capture well the structural features of polypeptides. In fact, the effective separation of the modular grains is of the same order of the natural coarse-graining provided by the separation of consecutive amino acids,  $a = 3.8$  Å, though this value is just indicative in this context where it is not known what fraction of the numerous prolines are in *cis/trans* conformations. Furthermore, the effective thickness of  $\Delta = 2.63 \pm 0.36$  Å is in excellent agreement with the one obtained by direct processing of several independent protein structures,  $\Delta \sim 2.7$  Å (38). Finally, we mention that the statistical significance ( $\chi^2$ ) of the TC fit is almost exactly the same as for the WLC. In this context the FJC is the worst performer since the associated  $\chi^2$  exceeds the TC or WLC one by a factor of two.

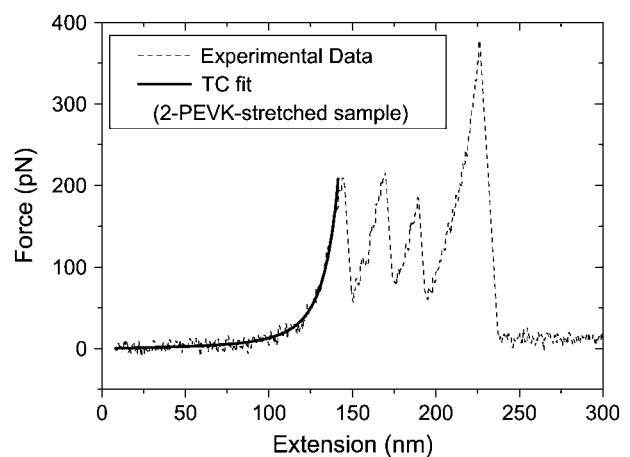


FIGURE 3 Typical fit of the PEVK stretching data through the TC model. The particular fit yields a contour length  $L_c = 147.6 \pm 0.3$  nm, a thickness  $\Delta = 0.34 \pm 0.01$  nm, and a granularity  $a = 0.45 \pm 0.02$  nm. For this set, the WLC provides a fit with a  $\chi^2$  analogous to that of the TC and yields  $L_c = 148.1 \pm 0.1$  nm and  $\xi_p = 0.76 \pm 0.02$  nm.

Another relevant class of biopolymers for which stretching measurements are available is constituted by polysaccharides, in particular cellulose, amylose, and dextran. We shall focus on cellulose since its stretching curve does not display the presence of the “bumps,” which in amylose and dextran denote the onset of structural transitions which can be captured only by atomistic models. On the contrary, cellulose, which is composed of sugar rings each spanning a distance of  $\sim 1$  nm, does not display dramatic structural changes upon stretching. For these reasons it is regarded as a standard example of entropic elasticity. It should be mentioned that, within traditional elastic models, the best fit of experimental data for forces up to 300 pN, is provided not by the WLC but by the FJC. In fact, under the working assumption of a constant error on the measured force (but also using an error proportional to the force), the FJC fit provides a  $\chi^2$  smaller than the WLC by more than 50%. The lengths of the statistical segments obtained from the FJC fit is  $l_K = 1.03 \pm 0.02$  nm, which is very close to the nominal lengths of the sugar units comprising cellulose. Consistent, the application of the TC model (Fig. 4) yields  $a = 1.02 \pm 0.01$  nm and  $\Delta = 0.54 \pm 0.02$  nm, which are both in agreement with the atomic structural parameters of cellulose.

Finally, we consider the case of dsDNA stretching. The extensive experimental data set used here was obtained by optical tweezers measurements on DNA in a PTC buffer (14). The type and concentration of the counterions in solution are known to affect strongly the strength (and even the sign) of the self-interaction of DNA molecules through the screening of the DNA phosphates (32,49,50). In a seminal study, Cozzarelli et al. described the effects of the self-repulsion of DNA in a solution containing monovalent counterions ( $\text{Na}^+$ ) in terms of an apparent DNA diameter (32). In their study, this effective diameter was recovered from the comparison of the knotting probabilities found experimentally for circular DNA

of known length with those predicted numerically for circular arrangements of a succession of cylinders. It was found that the effective diameter approached the bare-DNA one (2.5 nm) for high concentrations of counterions, whereas for low concentrations the poor electrostatic screening of the phosphates yielded much greater diameters, e.g., 15 nm in the presence of 10 mM  $\text{Na}^+$ . Our approach provides an alternative framework for the extraction of the effective DNA diameter which, furthermore, is inferred not from the analysis of structural properties in an equilibrium ensemble (as for the knotting probabilities) but from the elastic response of single molecules.

The good performance of the TC model (the fit is shown in Fig. 5) is highlighted by the very good value for  $\chi^2$ , which optimizes the fit. Even considering measurements up to forces of 25 pN (more than 650 data points), the  $\chi^2$  takes on the excellent value of 1.2. This constitutes a significant improvement among the class of inextensible chain models which are usually employed only up to forces of 10 pN. In fact, the performance of the inextensible WLC, both in its original and improved form, up to forces of 25 pN yields a value for  $\chi^2 > 2$ . Within the WLC scheme only through the addition of enthalpic effects which mimic the chain extensibility, is it possible to improve the quality of the fit reaching the value  $\chi^2 = 1.1$ . Incidentally, we mention that the FJC yields a poorer fit than the WLC or TC.

The fit through the TC model yields a contour length of  $1.335 \pm 0.001 \mu\text{m}$ , very close to the one recovered from the original WLC model  $1.327 \pm 0.001 \mu\text{m}$  (using forces up to 10 pN) or from the extensible WLC using forces up to 25 pN. The structural parameters extracted in this context are  $a = 3.27 \pm 0.57$  nm and  $\Delta = 5.76 \pm 0.58$  nm. They correspond to a persistence length of  $38.99 \pm 0.86$  nm, again consistent with, e.g., the one obtained from the improved WLC,  $\xi_p = 37.8 \pm 0.5$  nm. Consistent with the findings of Bouchiat et al. (5), the use of the extensible WLC model leads to a slightly larger persistence length,  $\xi_p = 40.6$  nm. Arguably,

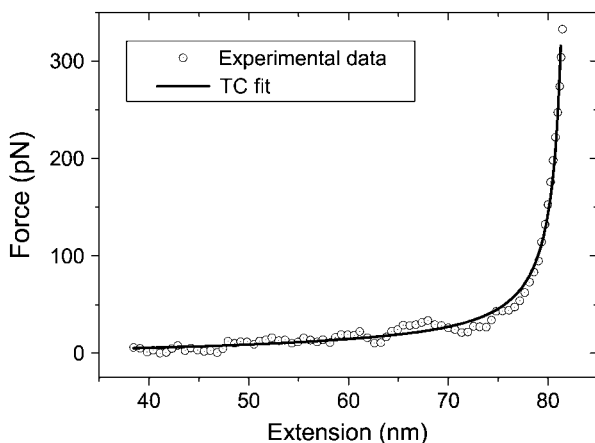


FIGURE 4 Fit of the cellulose stretching data through the TC model. The fit was carried out using forces up to 300 pN and yielded a contour length  $L_c = 82.35 \pm 0.02$  nm, a thickness  $\Delta = 0.54 \pm 0.02$  nm, and a granularity  $a = 1.02 \pm 0.01$  nm.

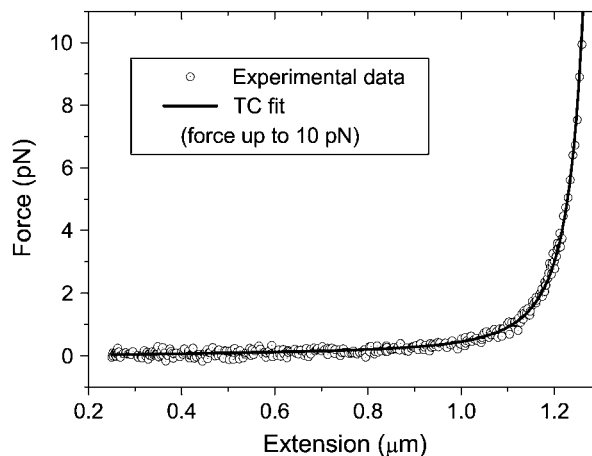


FIGURE 5 Fit of dsDNA stretching measurements through the TC model. Forces up to 10 pN were used.

the smaller  $\chi^2$  values obtained with the TC model may reflect the presence of an additional parameter with respect to the WLCs or FJCs. However, the increase of parameter space does not automatically lead to substantial improvements of the fits. If we were to refine the WLC model with its discretised version (45) whose parameters would then be the contour length, persistence length, and granularity, we would not improve the value of  $\chi^2$  obtained with the ordinary WLC model. The improvement obtained with the TC model can therefore be ascribed to the ability to capture in a better way the phenomenology of polymer stretching (in the same way that extensible models augment the range of applicability of inextensible ones).

The consistency of  $L_c$  and  $\xi_p$  with the data obtained from the WLC shows that the familiar elastic parameters of the chain are faithfully recovered by the TC model too. The additional insight obtained here is the indication of the effective DNA granularity and thickness. In fact, the value  $a = 3.27$  nm corresponds to  $\sim 9$  times the nominal basepair spacing in dsDNA, whereas the effective thickness, which corresponds to a diameter  $2\Delta \approx 11.5 \pm 1$  nm is  $\sim 5$  times the nominal hydration radius of dsDNA. A direct quantitative comparison of this value with the effective diameters found in Rybenkov et al. (32) cannot be made with this data set given the different type of solution employed. This comparison is, however, possible using a set of DNA stretching measurements done in the presence of sodium ions (2,51). Also in these cases, the TC model provides a better  $\chi^2$  than the FJC or WLC. It is found that in 10 mM  $\text{Na}^+$  the effective diameter is  $2\Delta = 23 \pm 3$  nm, which exceeds by 35% the estimate obtained by Cozzarelli et al. from the probability of occurrence of trefoil knotted DNA configurations. Given the diversity of the two approaches, it is pleasing that the two types of effective diameters are in fair quantitative agreement. Consistent with the intuitive expectations and the findings of Rybenkov et al. (32), it is found that at lower ionic strengths the effective diameter increases so that, e.g.,  $2\Delta = 51 \pm 7$  nm at 1.0 mM. Of all the cases considered here, the aspect that is least satisfactory is the order of magnitude difference between the effective spacing of the beads and the basepair separation. Although this consideration is mostly based on intuition, the good agreement of the effective bead spacings and nominal length of the “moduli” found for PEVK and polysaccharides suggests that a better consistency should be obtained for DNA too. This might be accomplished by considering, in addition to the thickness constraints, other important factors limiting the local freedom of the chain, such as introducing a bending or torsional rigidity term (see Marenduzzo et al. (52)) for a theoretical framework within which to consider these effects). Such extension of the TC model will be the object of future investigations.

## CONCLUSIONS

In summary, we have studied the feasibility of extracting the effective thickness and granularity of a biopolymer by fitting

its stretching response to that of a discrete thick polymer. The strategy that we followed relied on the preliminary numerical characterization of the elastic response of a TC through several Monte Carlo simulations. From the numerical results, we extracted a simple functional form for the force versus elongation curve as a function of effective thickness, chain granularity, and contour length. The resulting expression was used to analyze data coming from stretching experiments on the PEVK domain of proteins, cellulose, and double-stranded DNA in the presence of different concentrations of monovalent counterions. For all these biopolymers, we thus recovered, besides the persistence length (which is consistent with that obtained from standard entropic models), quantitative indications of their thickness and effective monomer size. These structural parameters turned out to be compatible with the nominal ones for the PEVK domain and cellulose or, in the case of DNA, with those previously obtained through a careful analysis of the proportion of knotted DNA molecules.

The results clarify that the use of suitable models allows us to extract from the experimental stretching curve not only some overall elastic phenomenological parameters but also fundamental structural properties of the polymer itself. This issue is not only a challenge in itself but has important experimental ramifications in the characterization of the polyelectrolytes self-interaction. The simple approach proposed here in terms of the TC model constitutes a novel effective scheme for characterizing the effective size of polyelectrolytes in various ionic solutions, starting from measurements of their elastic response.

We are indebted to S. Block, W. Linke, and P. Marszalek for providing us with the experimental data that were used in this study. We are grateful to E. Lattman, W. Linke, and A. Pastore for fruitful discussions.

This work was supported by the Istituto Nazionale Fisica della Materia.

## REFERENCES

1. Bustamante, C., Z. Bryant, and S. B. Smith. 2003. Ten years of tension: single-molecule DNA mechanics. *Nature*. 421:423–427.
2. Smith, S. B., L. Finzi, and C. Bustamante. 1992. Direct mechanical measurements of the elasticity of single DNA molecules by using magnetic beads. *Science*. 258:1122–1126.
3. Cluzel, P., A. Lebrun, C. Heller, R. Lavery, J.-L. Viovy, D. Chatenay, and F. Caron. 1996. DNA: an extensible molecule. *Science*. 271:792–794.
4. Strick, T. R., J.-F. Allemand, D. Bensimon, A. Bensimon, and V. Croquette. 1996. The elasticity of a single supercoiled DNA molecule. *Science*. 271:1835–1837.
5. Bouchiat, C., M. D. Wang, J. F. Allemand, T. Strick, S. M. Block, and V. Croquette. 1999. Estimating the persistence length of a worm-like chain molecule from force-extension measurements. *Biophys. J.* 76: 409–413.
6. Wenner, J. R., M. C. Williams, I. Rouzina, and V. A. Bloomfield. 2002. Salt dependence of the elasticity and overstretching transition of single DNA molecules. *Biophys. J.* 82:3160–3169.
7. Linke, W. A., M. Kulke, H. Li, S. Fujita-Becker, C. Neagoe, D. J. Manstein, M. Gautel, and J. M. Fernandez. 2002. PEVK domain of

- titin: an entropic spring with actin-binding properties. *J. Struct. Biol.* 137:194–205.
8. Li, H., W. Linke, A. Oberhauser, M. Carrion-Vazquez, J. Kerkvliet, H. Lu, P. Marszalek, and J. Fernandez. 2002. Reverse engineering of the giant muscle protein titin. *Nature*. 418:998–1002.
  9. Li, H., A. F. Oberhauser, S. D. Redick, M. Carrion-Vazquez, H. P. Erickson, and J. M. Fernandez. 2001. Multiple conformations of PEVK proteins detected by single-molecule techniques. *Proc. Natl. Acad. Sci. USA*. 98:10682–10686.
  10. Rief, M., J. Pascual, M. Saraste, and H. E. Gaub. 1999. Single molecule force spectroscopy of spectrin repeats: low unfolding forces in helix bundles. *J. Mol. Biol.* 286:553–561.
  11. Marszalek, P. E., A. F. Oberhauser, Y.-P. Pang, and J. M. Fernandez. 1998. Polysaccharide elasticity governed by chair-boat transitions of the glucopyranose ring. *Nature*. 396:661–664.
  12. Williams, P. M., S. B. Fowler, R. B. Best, J. L. Toca-Herrera, K. A. Scott, A. Steward, and J. Clarke. 2003. Hidden complexity in the mechanical properties of titin. *Nature*. 422:446–449.
  13. Best, R. B., S. B. Fowler, J. L. Toca-Herrera, A. Steward, E. Paci, and J. Clarke. 2003. Mechanical unfolding of a titin Ig domain: structure of transition state revealed by combining AFM, protein engineering and molecular dynamics simulations. *J. Mol. Biol.* 330:867–877.
  14. Wang, M. D., H. Yin, R. Landick, J. Gelles, and S. M. Block. 1997. Stretching DNA with optical tweezers. *Biophys. J.* 72:1335–1346.
  15. Boal, D. 2002. *Mechanics of the Cell*. Cambridge University Press, Cambridge.
  16. Pincus, P. 1976. Excluded volume effects and stretched polymer chains. *Macromolecules*. 9:386–388.
  17. Bustamante, C., J. F. Marko, E. D. Siggia, and S. Smith. 1994. Entropic elasticity of lambda-phage DNA. *Science*. 265:1599–1600.
  18. Cieplak, M., T. X. Hoang, and M. O. Robbins. 2002. *Proteins*. Folding and stretching in a Go-like model of titin. 49:114–124.
  19. Cieplak, M., T. X. Hoang, and M. O. Robbins. 2004. Stretching of proteins in the entropic limit. *Phys. Rev. E*. 69:011912.
  20. Gao, M., M. Wilmanns, and K. Schulten. 2002. Steered molecular dynamics studies of titin II domain unfolding. *Biophys. J.* 83:3435–3445.
  21. Marszalek, P. E., H. Lu, H. B. Li, M. Carrion-Vazquez, A. F. Oberhauser, K. Schulten, and J. M. Fernandez. 1999. Mechanical unfolding intermediates in titin modules. *Nature*. 402:100–103.
  22. Flory, P. 1989. *Statistical Mechanics of Chain Molecules*. Hanser Publisher, Munich.
  23. Marko, J. F., and E. D. Siggia. 1995. Stretching DNA. *Macromolecules*. 28:8759–8770.
  24. Hansen, P., and R. Podgornik. 2001. Wormlike chains in the large-d limit. *J. Chem. Phys.* 114:8637–8648.
  25. Buck, G., and J. Orloff. 1995. A simple energy function for knots. *Topol. Appl.* 61:205–214.
  26. Litherland, R., J. Simon, O. Durumeric, and E. Rawdon. 1999. Thickness of knots. *Topol. Appl.* 91:233–244.
  27. Gonzales, O., and J. H. Maddocks. Global curvature, thickness and the ideal shapes of knots. 1999. *Proc. Natl. Acad. Sci. USA*. 96:4769–4773.
  28. Katrich, V., W. K. Olson, P. Pieranski, J. Dubochet, and A. Stasiak. 1997. Properties of ideal composite knots. *Nature*. 388:148–151.
  29. Stasiak, A., and J. H. Maddocks. 2000. Best packing in proteins and DNA. *Nature*. 406:251–253.
  30. Maritan, A., C. Micheletti, A. Trovato, and J. R. Banavar. 2000. Optimal shapes of compact strings. *Nature*. 406:287–290.
  31. Marenduzzo, D., and C. Micheletti. 2003. Thermodynamics of DNA packaging inside a viral capsid: the role of DNA intrinsic thickness. *J. Mol. Biol.* 330:485–492.
  32. Rybenkov, V. V., N. R. Cozzarelli, and A. V. S. Vologodskii. 1993. Probability of DNA knotting and the effective diameter of the DNA double helix. *Proc. Natl. Acad. Sci. USA*. 90:5307–5311.
  33. Marszalek, P. E., Y.-P. Pang, H. Li, J. E. Yazal, A. F. Oberhauser, and J. M. Fernandez. 1999. Atomic levers control pyranose ring conformations. *Proc. Natl. Acad. Sci. USA*. 96:7894–7898.
  34. Marszalek, P. E., H. Li, and J. M. Fernandez. 2001. Fingerprinting polysaccharides with single-molecule atomic force microscopy. *Nat. Biotechnol.* 19:258–262.
  35. Rief, M., M. Gautel, F. Oesterhelt, J. Fernandez, and H. E. Gaub. 1997. Reversible unfolding of individual titin immunoglobulin domains by AFM. *Science*. 276:1109–1112.
  36. Buck, G. 1998. Four-thirds power law for knots and links. *Nature*. 392:238–239.
  37. Rawdon, E. 2000. Approximating smooth thickness. *J. Knot Theor. Ramif.* 9:113–145.
  38. Banavar, J., A. Maritan, C. Micheletti, and A. Trovato. 2002. Geometry and physics of proteins. *Proteins*. 47:315–322.
  39. Banavar, J. R., A. Flammini, D. Marenduzzo, and A. Maritan. 2003. Tubes near the edge of compactness and folded protein structures. *J. Phys. Condens. Matter*. 15:S1787–S1796.
  40. Premilat, S., and J. J. Hermans. 1973. Conformational statistics of short chains of poly(L-alanine) and poly(glycine) generated by Monte Carlo method and the partition functions of chains with constrained ends. *J. Chem. Phys.* 59:2602–2612.
  41. Flory, P. J., and V. W. C. Chang. 1976. Moments and distribution function for poly(dimethylsiloxane) chains of finite length. *Macromolecules*. 9:33–40.
  42. Lam, P.-M. 2002. Excluded volume effects in gene stretching. *Biopolymers*. 64:57–62.
  43. Livadaru, L., R. R. Netz, and H. J. Kreuzer. 2003. Stretching response of discrete semiflexible polymers. *Macromolecules*. 36:3732–3744.
  44. Storm, C., and P. C. Nelson. 2003. Theory of high-force DNA stretching and overstretching. *Phys. Rev. E*. 67:051906.
  45. Rosa, A., T. X. Hoang, D. Marenduzzo, and A. Maritan. 2003. Elasticity of semiflexible polymers with and without self-interactions. *Macromolecules*. 36:10095–10102.
  46. Lamura, A., T. W. Burkhardt, and G. Gompper. 2001. Semiflexible polymer in a uniform force field in two dimensions. *Phys. Rev. E*. 64:061801.
  47. Lee, G., W. Nowak, J. Jaroniec, Q. Zhang, and P. Marszalek. 2004. Molecular dynamics simulations of forced conformational transitions in 1,6-linked polysaccharides. *Biophys. J.* 87:1456–1465.
  48. Odijk, T. 1995. Stiff chains and filaments under tension. *Macromolecules*. 28:7016–7018.
  49. Odijk, T. 1998. Hexagonally packed DNA within bacteriophage T7 stabilized by curvature stress. *Biophys. J.* 75:1223–1227.
  50. Podgornik, R., P. Hansen, and V. Parsegian. 2000. Elastic moduli renormalization in self-interacting stretchable polyelectrolytes. *J. Chem. Phys.* 113:9343–9350.
  51. Lee, N., and D. Thirumalai. 1999. Stretching DNA: role of electrostatic interactions. *Eur. Phys. J. B*. 12:599–605.
  52. Marenduzzo, D., C. Micheletti, H. Seyed-allaei, A. Trovato, and A. Maritan. 2005. Continuum model for polymers with finite thickness. *J. Phys. A-Math. Gen.* 38:L277–L283.